Manuscript prepared for Nat. Hazards Earth Syst. Sci. Discuss.
with version 2014/07/29 7.12 Copernicus papers of the LaTeX class copernicus.cls.
Date: 17 November 2015

3-D-numerical approach to simulate the overtopping volume caused by an impulse wave comparable to an avalanche impact into a reservoir

R. Gabl, J. Seibl, B. Gems, and M. Aufleger

Unit of Hydraulic Engineering, University of Innsbruck, Technikerstr. 13, 6020 Innsbruck, Austria

Correspondence to: R. Gabl (roman.gabl@uibk.ac.at)

Abstract

The impact of an avalanche into a reservoir induces impulse waves, which pose a threat to population and infrastructure. For a good approximation of the generated wave height and length as well as the resulting overtopping volume over structures and dams, formulas, which base on different simplifying assumptions, can be used. Further project-specific investigations by means of a scale model test or numerical simulations are advisable for complex reservoirs as well as the inclusion of hydraulic structures such as spillways.

This paper presents a new approach for a 3-D-numerical simulation of an avalanche impact into a reservoir. In this model concept the energy and mass of the avalanche are represented by accelerated water on the actual hill slope. Instead of snow, only water and air are used to simulate the moving avalanche with the software FLOW-3D. A significant advantage of this assumption is the self-adaptation of the model avalanche onto the terrain. In order to reach good comparability of the results with existing research at ETH Zürich, a simplified reservoir geometry is investigated. Thus, a reference case has been analysed including a variation of three geometry parameters (still water depth in the reservoir, freeboard of the dam and reservoir width). There was a a good agreement of the overtopping volume at the dam between the presented 3-D-numerical approach and the literature equations. Nevertheless, an extended parameter variation as well as a comparison with natural data should be considered as further research topics.

1 Introduction

Avalanches are dangerous natural events that can threaten settlements, roads or other infrastructure objects in mountainous regions (Grêt-Regamey and Straub, 2006). In the Alps, with their many large alpine reservoirs for hydropower generation, the impact of avalanches into reservoirs can have a great effect. An avalanche impact, but also rockfalls, landslides or cold volcanic mass flows (Akgün, 2011; Mohammed and Fritz, 2012; Waythomas et al., 2006) may generate impulse waves, which can overtop water-

retaining structures and even cause a massive failure in case of an earth-fill dam. Especially landslide-induced impulse waves are known to have caused great destruction in the past. In particular the catastrophe at the Vajont reservoir in Italy in 1963 (Panizzo et al., 2005a, b) and the incident in Lituya Bay in Alaska in 1958 (Fritz et al., 2009; Zweifel, 2004) have to be mentioned. A collection of historical avalanche-induced impulse waves has been compiled by Müller (1995).

Once the avalanche reaches the water surface of the reservoir, the complete impacting process can be divided into two parts: (a) the generation and the movement of the avalanche and (b) the impact into the reservoir with the propagation of the impulse wave. Different types of special numerical software are available to simulate the first part (Sect. 2.1). These investigations are used for a wide range of different risk analyses and in case of a reservoir, which is on the avalanche track, further modelling concepts for the impulse wave are needed. The paper will focus on these processes in the reservoir with the help of three-dimensional (3-D) numerical simulations.

Based on the characteristics of the avalanche-induced impulse waves, the process within the reservoir can be divided into three phases: (a) the wave generation including the impact of the sliding mass, (b) the wave propagation in connection with lateral propagation including the progressive frequency dispersion and (c) the last phase, which is the run-up on the (opposite) shore. The transition between these three phases is smooth. If the distance between impact spot and the accumulation areas is very small, the propagation phase of avalanche induced impulse waves can sometimes be neglected (Zweifel, 2004).

2 Modelling concepts

2.1 Avalanche simulation

The formation and movement of avalanches can be simulated using several existing software solutions. One commonly applied numerical tool is the RAMMS (rapid mass movement system) software, which is used by the WSL (Swiss Federal Institute for

Forest, Snow and Landscape Research), Institute for Snow and Avalanche Research SLF (Christen et al., 2010; Teich et al., 2014). In Austria the SAMOS-AT (Sailer et al., 2002; Sampl and Zwinger, 2004) and ELBA (Energy Line Based Avalanche) (Volk and Kleemayr, 1999) are well known examples of software (Keiler et al., 2006) and used by the BFW (Federal Research and Training Centre for Forests, Natural Hazards and Landscape, Department of Natural Hazards and Alpine Timberline) and other institutions. These tools link meteorological data with terrain information for the generation of avalanches and use different modelling concepts for the movement. A simulation provides mass, hight and velocity of the avalanche depending on the time and the location as an input dataset for hazard assessment. These parameters are used as an input for further simulation of an avalanche impact into a reservoir to calibrate the modelling assumption of the avalanche.

2.2 Scale model test

The investigation of an avalanche impact and the thereby generated impulse wave in a reservoir can not be simulated with the numerical tools presented in Sect. 2.1. Therefore, further modelling concepts are needed, which are based on laboratory experiments or numerical investigations. The latter approach will be addressed in Sect. 2.4.

The build up of a scale model test is a very reliable but also cost-intensive way to evaluate the danger of impulse waves in reservoirs caused by avalanches. In addition to general scale effects (Heller, 2011), the critical aspect for the definition of the used scale is the minimal water depth in the model, which should not be less than 0.2 m (Heller, 2008; Heller et al., 2008a). The input parameters provided by the avalanche simulation (typically the location of the impact, mass, velocity, slide height) are implemented based on scaling laws (Froude similarity). Therefore, different concepts for the model avalanche can be used to obtain the needed impulse, which is the result of mass multiplied by velocity. In exemplary experiments, sandbags on wheels (similar to a skate board), slides with different front angles or granulates have been accelerated in a chute to simulate such an impacting avalanche (Gabl et al., 2014b; Heller and Spinneken, 2013; Rastello et al., 2002). All these

assumptions are simplifications, that can hardly be calibrated because of the lack of field data.

In recent years, extensive basic research in the field of avalanche and landslide induced impulse waves in reservoirs have been carried out at ETH Zürich. Within these laboratory tests, different granulates and solid bodies were used. In the following section a brief overview is given, leading to approaches to calculate the impulse wave (behaviour, height, length) and the overflow volume depending on the actual dam structure (Sect. 2.3).

Different studies have accurately shown the impact phase of wave generation using scale model tests (Fritz, 2002; Fritz et al., 2003a, b, 2004; Fuchs et al., 2013). These impact tests focus on subaerial landslides and distinguish between unseparated and separated flow depending on the slide Froude number. The flow separation occurs at high impact velocities, when the water in the reservoir is prohibited to flow backwards over the impacting body. The run-up and overtopping were investigated by Müller (1995) with the help of scale-model tests. Regarding the process of run-up, mass-included impulse waves are similar to tsunamis insofar as they also occur as surging breakers. Müller (1995) developed formulas for the run-up height and the volume of water that overtops the dam depending on the slope angle. Furthermore, the influence of ice cover on the impact and the propagation of the impulse waves were investigated, which led to the conclusion that the influence of the ice cover on the wave height can be completely neglected up to 0.5 m thickness.

Zweifel (2004) focused on the effects of slide density and water depth on the impulse wave. It has been shown that the impact-Froude number, which can be regarded as dimensionless slide velocity, is the dominant slide parameter. A higher impact speed generates a greater maximum amplitude of the primary wave in case of larger slide densities than water. For tests with a slide density smaller than the density of water (characteristic for snow), only a minor influence of the impact speed could be found. Zweifel (2004) shows that the slide thickness has a strong influence on the maximum amplitude at slide densities smaller than the water density. In case of a larger slide density, there is no clear correlation between the maximum amplitude and the slide thickness. At low densities the slide volume, and thus the sliding mass, affects the maximum amplitude.

Heller (2008) extended the existing investigation on the influence of the seven governing parameters, which included the still water depth h, the slide thickness s, the slide impact velocity v_s, the bulk slide volume V_s, the bulk slide density ρ_s, the slide impact angle α and the grain diameter, and analysed the wave generation process based on those parameters. The results of all studies (scale model tests and further numerical simulations) were summarised as simplified formulas (Heller et al., 2009 based on Heller et al., 2008b).These key expressions have been used to validate the presented simplified 3-D-numerical investigations and will be listed in Sect. 2.3.

The above mentioned experiments at ETH Zürich (Fritz, 2002; Fuchs et al., 2013; Heller, 2008; Zweifel, 2004) were conducted in a rectangular prismatic wave channel with a slope ramp, with variable steepness. The used channel has a length of 11 m, a height of 1 m and a width of 0.5 m. The main investigation section focused on the channel axis (Heller, 2008), but not only basic experiments were performed. Fritz et al. (2009) simulated the incident at Lituya Bay in Alaska 1958 at scale of $1:675$ in the two dimensional wave-channel of ETH Zürich and also in a three-dimensional model at scale of $1:400$. Fuchs et al. (2011) experimentally investigated avalanche- and rockfall-induced impulse waves at the storage Kühtai in Austria (scale $1:130$). Further project-specific examples of scale model tests to investigate impulse waves can be found in Di Risio et al. (2009); Gabl et al. (2010); Heller and Spinneken (2015); Mohammed and Fritz (2012); Müller (1995); Panizzo et al. (2005a) and Panizzo et al. (2005b).

2.3 Formulas to calculate the overtopping volume

The overtopping volume per m crest length V [$m^3\,m^{-1}$] is one of the main parameter for risk analysis of an avalanche impact into a reservoir. Hence, this parameter is used for the comparison of the presented 3-D-numerical simulations with FLOW-3D and the given basic equations by Heller et al. (2009, 2008b) respectively. To calculate this parameter as shown in Eq. (7) some further equations are needed. First, the impulse product parameter P [–] is

calculated:

$$P = \frac{v_s}{\sqrt{g \cdot h}} \cdot \left(\frac{s}{h}\right)^{1/2} \cdot \left(\frac{\rho_s \cdot V_s}{\rho_w \cdot b \cdot h^2}\right)^{1/4} \cdot \left[\cos\left(\frac{6}{7} \cdot \alpha\right)\right]^{1/2} \quad (1)$$

The value P is made up of five parameters of the avalanche itself (namely the slide impact velocity v_s [m s^{-1}], the bulk slide density ρ_s [kg m^{-3}], the bulk slide volume V_s [m^3], the slide width b [m] and the slide thickness s [m]), further the still water depth h [m], the slide impact angle α [°], the water density ρ_w [kg m^{-3}] and the gravitational acceleration g [m s^{-2}] are also considered. Based on P, the wave height $H(x)$ [m], the wave period $T(x)$ [s] and the wave length L [m] can be computed as follows with x [m] as the streamwise coordinate in the longitudinal channel direction and the solitary wave celerity $c(x)$ [m s^{-1}]:

$$H(x) = \frac{3}{4} \cdot \left[P \cdot \left(\frac{x}{h}\right)^{-1/3}\right]^{4/5} \cdot h \quad (2)$$

$$T(x) = 9 \cdot P^{1/4} \cdot \left(\frac{x}{h}\right)^{5/16} \cdot \left(\frac{h}{g}\right)^{1/2} \quad (3)$$

$$L(x) = T(x) \cdot c(x) \quad (4)$$

Subsequently, the run-up height R [m] and the overtopping volume V_0 [m^3 m^{-1}] (with a zero freeboard f [m]) can be defined as follows:

$$R = 1.25 \cdot \left(\frac{H}{h}\right)^{5/4} \cdot \left(\frac{H}{L}\right)^{-3/20} \cdot \left(\frac{90°}{\beta}\right)^{1/5} \cdot h \quad (5)$$

$$V_0 = 1.45 \cdot \kappa \cdot \left(\frac{H}{h}\right)^{4/3} \cdot \left(\frac{T}{(h/g)^{0.5}}\right)^{4/9} \cdot h^2 \quad (6)$$

Therefore, Eqs. (2)–(4) are evaluated in front of the dam and two additional parameters have to be specified: the run-up angle equal to the dam face slope β [°] and the overfall coefficient

κ [–] based on the formula of Poleni. For an existing freeboard f, the overtopping volume V_0 is reduced to V [m^3 m^{-1}] with the following equation:

$$V = \left(1 - \frac{f}{R}\right)^{11/5} \cdot V_0 \tag{7}$$

All presented equations and further information about the specific use can be found in Heller et al. (2009). The entire simplified calculation can be carried out with an Excel-Tool provided by ETH Zürich (http://www.vaw.ethz.ch/publications/vaw_reports/2000-2009). This tool is also used in this paper for the comparison with the 3-D-numerical simulations (Sect. 4).

The formulas are based on different generalisations and simplifications. To use them for a specific adaptation on a complex bathymetry or the consideration of wave reflection, the applicability of these formulas has to be carefully checked (Akgün, 2011). In the presented case, these formulas are compared with the 3-D-numerical simulation, in which the avalanche is implemented with a new approach based on inflowing water instead of snow. Therefore, a simplified geometry is investigated to reach a good comparability (Sect. 3.3).

2.4 Numerical simulations

In addition to (existing) scale model tests, more and more numerical models are used, for which free surface modelling (interaction of water and air) is a standard application. Heller et al. (2009) also lists further numerical investigations in the context of research gaps. High potential can be especially seen in meshless methods, namely the smoothed particle hydrodynamic (SPH). Therefore, the fluid is discretised with particles, which can move in respect of a kernel-smoothed influence of its neighbourhood (Capone et al., 2010; Cascini et al., 2014; Dai et al., 2014; Meister et al., 2014). The SPH-standard procedure for wall boundaries is the use of immobile ghost particles, which can be easily applied for plain surfaces. The implementation of a complex geometry and surface roughness are current issues of research (Ferrand et al., 2013).

Examples for existing two-dimensional (2-D) simulations of scale model tests can be found in Zweifel et al. (2007) and Ataie-Ashtiani and Yavari-Ramshe (2011). Ataie-Ashtiani and Shobeyri (2008) and Shan and Zhao (2014) also presented numerical simulations of impulse waves, which focus purely on the impact of objects in water. Dalban Canassy et al. (2011) investigated the effects of an impact caused by the calving of the Triftgletscher into a glacial lake in Switzerland. Waythomas et al. (2006) operated a 2-D-numerical tsunami simulation induced by an eruption of the Augustine volcano in Alaska.

A 3-D-numerical approach should be used especially for complex terrain, smaller reservoirs and if the effect of spillways or other structures should be considered. While conducting a broad scale model test of a weir and intake structure, Gabl et al. (2014b) used the investigation of an avalanche impact into a reservoir of a diversion plant in the Austrian Alps as a validation experiment for 3-D-numerical simulations. The simplified model assumptions of the laboratory test could be very accurately reproduced with 3-D-numerical simulation (FLOW-3D). In this particular case, moving solids and a combination of water and particles are accelerated in the same manner as in the scale model test. For the impacting solid body only a prescribed motion could be used, because the coupled mode lead to unrealistic bouncing, as soon as the moving object touches the water surface. Hence, the mass conservation after the impact was hard to achieve. The challenge of the particle assumption is, that FLOW-3D simulates a full interaction of particles with everything else but not with each other. Therefore, additional water is needed to control the behaviour of the particles in the chute. Nevertheless, the main conclusion of this work was that the differences between the result of the scale model test and the numerical simulation are far smaller than the uncertainties of different modelling assumptions for the avalanche (Gabl et al., 2014b). In general, the prediction of the governing avalanche parameter as an extreme event is hard to verify. However, Sect. 3.1 presents a new concept, which can be used for a better implementation of a specific avalanche in a 3-D-numerical model.

3 Methodology

3.1 Adapted implementation of an avalanche

For both modelling concepts (scale model test and numerical simulation), two assumptions are frequently used: (a) the impacting avalanche is homogeneous and (b) the impact is limited to a specific location in the reservoir. Depending on the used modelling concept for the avalanche, this latter assumption can lead to very different results. If for example simple solid slide is used, it results in a single, big impact at a defined place on the water surface. A good adaptation of the model avalanche to an actual terrain can be achieved by using granulates (Fuchs et al., 2011). To implement a comparable model into 3-D-numerics, the simulation of three fluids would be necessary: air, water and snow. Some 3-D-numerical simulation programs, such as FLOW-3D, are limited to two fluids, that can be computed simultaneously. In order to profit from the advantages of this software, which allows for a fast and accurate simulation of unsteady free surface flows (Flow Science, Inc., 2014; Hirt and Nichols, 1981), a modelling approach for the avalanche containing only two fluids is necessary.

Based on third-party funded research at the Unit of Hydraulic Engineering at the University of Innsbruck, different concepts were studied. The starting point was the use of moving objects, which represent the avalanche as a solid with a defined velocity. These bodies and also the particles were accelerated in a chute. The main goal was to reproduce an existing scale model test, which would be focused on the concentrated impact and the conditions at a weir structure (Gabl et al., 2014b). It was necessary to find a new concept to simulate more complex avalanches – in particular to enhance the impact assumption – in order to get away from an only local concentration given by the simple acceleration in a chute. One possible way, which has already been tested in different projects, is the replacement of the snow with water. The following steps represent the general work-flow for this concept:

1. An avalanche study that has been conducted with a suitable software (examples for these kinds of software are mentioned in Sect. 2.1) provides the critical avalanche track and further required input parameters. For this investigation, the avalanche must be simulated based on an empty reservoir. Before the avalanche reaches the water surface, a specific control section is defined. This is the connection between the simulation of the avalanche and the further investigation of the impact and the water movement in the reservoir. For the latter, the software FLOW-3D is used, but the concept can be adapted for different products.

2. Based on the results of the avalanche simulation, a mass-equivalent amount of water is placed in the starting zone of the avalanche, for which the chosen water depth should be adjusted in relation to the distribution of the snow heights. In general, the slide density ρ_s and the bulk slide volume V_s are only used in Eq. (1) to calculate the impulse product parameter P. If the slide density is increased (change from snow with approximately 330 kg m^{-3} to ρ_w with 1000 kg m^{-3}) the used bulk slide volume has to be decreased with the same factor to simulate the same P. Based on these initial conditions, the 3-D-numerical simulation is started and the water flows down the avalanche track.

3. At the control section, the kinetic energy or rather the momentum (product of the mass and velocity) of the incoming water is compared to the previously simulated avalanche in step 1 over the entire impact time. In general, the water has a higher density than snow and so the water avalanche is too fast.

4. To correct this effect, a restart simulation on the existing simulation is conducted. After some simulated seconds, the complete water body of the avalanche model is used as an initial condition for a restart. The thereby chosen time is only a first assumption and lasts typically 2– 4 s. The only difference between the original simulation and the restart is, that the velocity is set to zero at the beginning of the restart simulation (Fig. 1a). Hence, the kinetic energy of the impacting water is reduced, but the influence of the terrain on the model avalanche is maintained. This is the main advantage in

comparison to a user defined starting point of the water at a lower level than the starting zone.

5. In order to calibrate the velocity of the model avalanche at the moment of impact, it is evaluated at the control section (identical to step 3) and, if necessary, the time of the restart is changed accordingly. Depending on the terrain and the avalanche characteristics, with approximately three to four iterations a good avalanche model in FLOW-3D can be build up, which should be comparable in expansion and fragmentation to the original simulated avalanche (step 1).

6. After this process, the impacting mass, shape and velocity of the model avalanche is comparable to the avalanche computed in step 1. The main difference is the reduced slide thickness s, which is also used to calculate the impulse product parameter P as shown in Eq. (1). To quantify the influence of this assumption, a parameter study of this value based on the equations (Heller et al., 2009) should be conducted. The water distribution in the release zone should be varied to make sure that the chosen distribution has a negligible influence on the results. Therefore, a high decoupling of user-specified input can be reached for the model avalanche. Further studies, especially for the roughness of the terrain should be considered as well. All these investigations should be part of a global sensitivity analysis, which includes the complete input parameters as it is advised by Heller et al. (2009).

The result of the shown process is a model avalanche based on water, which is the boundary condition for the impulse wave in the reservoir. By use of the 3-D-numerical simulation, the complex reflection and interaction of the impulse wave can be calculated. Furthermore, spillways or other structures, such as bridges or wave breaker, can be implemented in the 3-D-numerics.

In addition to the self-adaptation of the thereby generated model avalanche onto the given terrain, another advantage is the mass conservation. Both characteristics can not be easily implemented in a solid body concept with a fixed moving part. The difference in density between snow and water is compensated by correcting the used bulk slide volume

V_s. Thus, the momentum of the impact remains the same. Furthermore, the slide impact velocity v_s and the expansion of the model avalanche in FLOW-3D is comparable to the original simulated avalanche. The model avalanche, which has been calibrated at the time-step before the impact, can reproduce the given avalanche parameters over the complete inflowing time very accurately. A disadvantage is that the slide thickness s of the model avalanche is reduced because of the different density. In addition, this assumption assumes that the avalanche has immediately melted since only liquid water is used. The influence of the packed snow in the impact area on the (reflected) impulse wave has thereby to be neglected.

Figure 1 exemplarly shows three time steps of one calibration simulation (step 4). For this particular case, a 150-year avalanche was simulated, which is in accordance with design event intensities in torrent and avalanche hazard management and zone mapping in Austria (Hübl et al., 2011). As part of the verification, a 300-year avalanche was also tested. For such extreme events, no calibration data is commonly available. Because of the protection of data privacy no further results of realistic examples will be published. Nevertheless, the aim of this paper is to evaluate the adapted concept for the presented implementation of an avalanche. Therefore, a simplified model, presented in Sect. 3.3, is used for comparison with the existing formulas, which are summarised in Sect. 2.3. In this particular case the adaptation of the model avalanche on a terrain is not needed and the investigation is only a proof of the concept itself.

3.2 Software

The numerical calculations are performed with FLOW-3D. This 3-D-numerical software is a good solution for flow calculation with a free surface and is based on the Reynolds-averaged Navier–Stokes (RANS) equations in combination with the Volume of Fluid (VOF) technique (Flow Science, Inc., 2014; Hirt and Nichols, 1981). The software works with mesh blocks based on orthogonal rectangular grids, which are very easy to generate and compute. The use of structured, rectangular cells leads to the numerical advantage that all indices for neighbouring elements are known and no additional neighbour list has to be

stored. In contrast to body-fitted coordinate elements, a solid surface can cut through an element as a plane in FLOW-3D (Flow Science, Inc., 2014; Gabl et al., 2014a). The original geometry is modified based on the chosen grid. Hence, there is no need for a constant adaptation of the grid to model a moving object. This characteristic of FLOW-3D can be used for the implementation of moving gates (Dargahi, 2010), dam failures (Seibl et al., 2014) or moving solid avalanches (Gabl et al., 2010, 2014b).

In case of a sharp interface, FLOW-3D calculates, based on the VOF, the surface slope in each cell. As a result of the used modelling concepts, only the velocities of the water (fluid 1) have to be computed and the second fluid (in general air) is not considered. The solver is very accurate and stable for free-surface simulations. Various validation experiments showed the capacity of FLOW-3D. As examples, the software was successfully used for the investigation of a combined sewer overflow (Fach et al., 2009) and spillways (Gabl et al., 2014a; Johnson and Savage, 2006) as well as an analysis tool for bed-load transport processes and flood protection (Gems et al., 2014). The software was also successfully used for local refinements of bridges (Erduran et al., 2012) or air entrainment caused by a vortex (Lo et al., 2015).

3.3 Model setting

The basic scale model tests at ETH Zürich base on investigations conducted in a channel with a length to width ratio η of 22 [–] ($= L_R/B = 11\,\text{m} \ / \ 0.5\,\text{m}$). The inclination of the slope ramp was varied between 30 and 90° and different granular slide materials were tested (Sect. 2.2). In contrast to these laboratory tests, the presented work uses a more complex natural scale geometry for the 3D-numerical simulations with FLOW-3D. Therefore, the main goal of the investigation is not to reproduce the laboratory experiments comparable to Gabl et al. (2014b). Moreover, the given equations, which are the results of these tests at ETH Zürich (Sect. 2.3), are used to validate the avalanche concept based on water. The hereafter presented and in Tab. 1 summarised parameters for the simplified geometry are chosen in reference to an actual project. The complete numerical study is split into two parts. First a reference set-up is investigated in Sect. 4.1. Based on this simulation,

variations of geometrical parameters, namely freeboard f, still water depth h, dam height h_D and the width of the channel B are investigated (Sect. 4.2). The latter is used to analyse the influence of the different parameters on the results.

The reference geometry is shown in Fig. 2 and the key input parameters are summarised in Table 1. The chosen set-up consists of a rectangular channel ($B = 80$ m) with a simplified vertical concrete-dam (dam face slope $\beta = 90°$) and an outflow boundary condition behind this structure. The crest width of the dam b_k is fixed with 3 m. At the opposite end of the model, an inclined ramp ($\alpha = 40°$) is placed as flow path for the model avalanche. The slide width b of the model avalanche is equal to the width of the channel. Both sides of the channel are modelled with a solid wall. All surfaces are used with no additional roughness. For the presented numerical simulations the standard k-ϵ-turbulence model is used.

The origin of the coordinate system is defined in the middle of the bottom line of the upstream dam. The z-axis is fixed in the opposite direction to gravity. The positive x axis of the local coordinate system, which is used for the simulation, points in the same direction as the horizontal part of impact velocity and is labelled as $\tilde{x}$. Because of the inclined slope, the impact point of the avalanche into the reservoir, for which the value x is equal to 0 [m], is depending on the still water depth h (Fig. 2). The reference calculation is based on a still water depth h of 30 m and a freeboard f of 2 m. Corresponding to these values, the dam height h_D is 32 m in total. The distance L_R between the impact point and the water-side of the dam is 656 m for the reference case. Consequently, the value x, which is needed for the equations in Sect. 2.3, is defined as $x = \tilde{x} - 656$ [m] for this water depth. The division of length $L_R = 656$ m and width $B = 80$ m of the chosen reservoir leads to a ratio η of 8.2 [–], which is smaller than the value for the model test at ETH Zürich. To reach the same η value of 22 [–] the width of the channel B should be equal to 30 m. This value has no main influence on the results, if the 3-D-effects can be neglected. The variation of the parameter B is part of the variation in Sect. 4.2.

The simulations with the software FLOW-3D are based on one single mesh block with a homogeneous cell size of 1 m in each direction. Approximately 5.4 million of the total number of requested cells (nearly 10 million) are active in the calculation. The other cells

are blocked by solids. The reference case is also simulated with a cell size of 0.5 m, which shows nearly no difference in the results (water level, overtopping volume, local velocities). Hence, the shown results are independent of the chosen mesh. For the variation of the reservoir width B in Sect. 4.2, the mesh is extended with the same cell size.

4 Results

4.1 Reference case

4.1.1 Impact of the model avalanche

At the upper end of the slope, a water block with a chosen volume V_s of 36 150 m^3 is positioned, which represents the model avalanche. For this water and the filling of the reservoir, the initial speed v_0 is set to 0 $m\,s^{-1}$, each with a hydrostatic initial pressure distribution. By starting the simulation, the water is accelerated by gravity ($g_z = -9.81\,m\,s^{-2}$) and reaches a velocity of approximately 40 $m\,s^{-1}$ at the impact into the reservoir (Fig. 3, left column). No additional calibration step, as presented in Sect. 3.1, is conducted for these simplified investigations. Adding the entire impact volume without the consideration of losses over the dam and assuming zero flow velocities in the reservoir, the water level in the reservoir would raise about 0.69 m, which is 34 % of the available freeboard.

The investigation of the impulse wave shows that the primary wave front is nearly parallel to the dam and orthogonal to the wall. This is comparable to the laboratory tests at ETH Zürich (Sect. 2.2). In cases, in which the slide width b is equal to the channel width B or essentially no 3-D-effects are expected, the analysis can be simplified to a 2-D-problem. To qualify the mixture process, Fig. 4 shows a 2-D-section of the symmetry plane. Thereby, a tracer is added to the inflowing water, which is used to colour the impacting water red. This additional parameter is shown as blue for the water in the reservoir. All colours between these two boundaries mark different stages of the mixing. These analyses show that the

model avalanche stays stable nearly down to the bottom of the reservoir (still water depth $h = 30\,\text{m}$), which can be compared well with the impact behaviour of artificial granular material shown by Fritz et al. (2003a).

To classify the impact behaviour, the Froude number of the inflowing water is analysed with FLOW-3D. Depending on the location and time, the Froude number is approximately in the range of 7–8 [–] for the chosen set-up. According to Fritz et al. (2003b), who used a higher bulk slide density ρ_s of 1620 $\text{kg}\,\text{m}^{-3}$ in his experiments, Froude numbers bigger than 4 [–] lead to an outward collapsing impact crater. Figure 3 shows in its left column six time-steps starting after the first interaction of the model avalanche with the reservoir (starting at second 5.6 of the simulation with a Δt of 1 s between each picture). The velocity magnitude is used for the colour scale with an upper limit of 40 $\text{m}\,\text{s}^{-1}$. The vectors indicate the local flow direction. These analyses show a small outward collapsing impact crater in the first seconds, but afterwards it converts into a backward collapsing impact crater. This behaviour also has great similarities to the studies of Fritz et al. (2003b).

The resulting impulse wave in the reservoir is best described as a solitary wave. It is characterised by large mass transport, no wave through and an approximate wave length of $L = \infty$. The water particles move mainly horizontally (Fig. 3, right column, first picture). Theoretically, this wave should break once if it reaches a wave height H bigger than $0.78 \cdot h$ (Heller, 2008; Heller et al., 2009; Müller, 1995; Zweifel, 2004). In the presented reference case, H reaches approximately $0.57 \cdot h$ and consequently no breaking of the wave can be observed.

4.1.2 Overtopping at the dam

The overflow process at the dam is described in detail by Müller (1995) and a benchmark test of a wave running over an inclined dam body is presented by Fuchs et al. (2010) and Fuchs and Hager (2012, 2015). To reduce the complexity, a vertical dam ($\beta = 90°$), which is similar to the upstream face of a gravity dam, is investigated in this study. The processes behind the dam are not considered for this particular case. For real application, the water distribution and potentially dangerous velocities, which can lead to an erosion downstream

of the dam, could also be identified by use of a 3-D-numerical simulation. Figure 3 shows in the right column six time steps of the overtopping of the primary wave at the dam. The fluid is coloured by the x velocity and the scale is limited to 10 m s^{-1}. To analyse the time dependence of the overtopping flow, a section 0.5 m before the middle of the dam crest is used to define it on junctions of the cells (flow exchange is monitored between the cells). After 36 s the first wave overtops at this section and the maximum is reached approximately 38 s after the simulation starts.

The Excel-Tool based on Heller et al. (2009) and provided by ETH Zürich is used to compare the results of the simulation with FLOW-3D. The input parameters for this tool are listed in Table 1. The chosen slide impact velocity v_s and slide thickness s are based on evaluation of the FLOW-3D simulation at the time-step just before the model avalanche reaches the reservoir. The used value v_s is the mean value of the depth-average velocity over the entire front section of the model avalanche, which is used to calibrate the model avalanche in the proposed concept (Sec. 3.1). This is a simplification in comparison to Heller et al. (2009), who use the side centroid impact velocity of the impacting avalanche. To find s, the maximum of the vertical flow depth at this timestep is multiplied with cos(40°) to get the orthogonal value on the slope.

Based on this mentioned input parameter and the assumption of a 2-D-case, the Excel-Tool calculates an overtopping volume V per m crest length of 431.2 m^3 m^{-1}. This primary wave reaches the dam 27.5 s after the impact. Figure 5 shows the accumulation of the overtopping volume over time depending on the definition of Heller et al. (2009). Therefore, the starting time t is set to 0 s, when the slide front reaches the still water surface (time of the 3-D-numerics minus 4.6 s). The primary wave of the 3-D-numerical simulation overflows the dam, depending on the chosen moment (first wetting of the control section or reaching the maximum at the control section), 4 to 6 s later than calculated with the Excel-Tool. The overtopping volume V of the primary wave for the 3-D-numerical simulation (486.8 m^3 m^{-1}) is only 13 % larger than the calculated value based on Heller et al. (2009).

A larger run-up height R is observed in FLOW-3D with 15.7 m (equal to a maximum overtopping height of 13.7 m at the dam including 2 m freeboard) compared to 15.2 m based

on the Excel-Tool. This increased value leads subsequently to a higher overtopping volume V.

The same overtopping volume V of the 3-D-numerics can be reached with the Excel-Tool if the input parameter v_s is increased by 9 % or, as a second option, the evaluated slide thickness s by 18 %. To evaluate this difference, a variation of input parameters is conducted and presented in Sect. 4.2.

The 3-D-numerical simulation monitors the resulting overtopping volume over 1000 s. Beside the primary wave, which is in general most critical, further waves caused by reflections and interactions overtop the dam. They lead to a total overtopping volume $V_{1000\,s}$ of 898.7 $m^3\,m^{-1}$, which is an increase of 84 % of the preliminary wave. The accumulated overtopping volume can be approximated by a logarithmic trendline ($R^2 = 0.9961$). These reflected waves, which are depending on the reservoir shape, can have a significant impact.

4.2 Parameter variation

4.2.1 Concept

The input parameters for the computation of the overtopping volume V can be categorised as follows: (a) avalanche or slide values (for example slide impact velocity v_s, density ρ_s or slide thickness s) and (b) geometrical parameters, like the still water depth h, freeboard f and the width of the reservoir B. As shown in Sect. 4.1, the first mentioned group of parameters are chosen based on the 3-D-numerical simulation for this particular case. For an actual project, an avalanche model can provide these values. The implementation of a sensitivity analysis for these particular inputs is a standard procedure and advisable (Heller et al., 2009). The geometrical informations are in general fixed values and have a big influence on the overtopping volume V. The first step of the conducted parameter study focuses on the combination of freeboard f and still water depth h (Sect. 4.2.2, Tab. 2). Furthermore, the width of the dam B in relation to the impact slide width b of the avalanche model is investigated. With the latter simulations, presented in Sect. 4.2.3, the transition

of the 2-D to a 3-D-case is investigated. The presented variations are only exemplary and make no claim to be complete.

4.2.2 Freeboard and still water depth

In the formulas presented in Sect. 2.3, the freeboard f is only used as a reduction factor in Eq. (7). In contrast to this, nearly all computed parameters depend on the water depth h. For the reference case, these two values are fixed with $f = 2\,\text{m}$ and $h = 30\,\text{m}$ and lead to a dam height $h_\text{D} = 32\,\text{m}$. As a first part of the parameter study, the freeboard f is held constant at a value of 2 m and the still water depth h is varied. Consequently, the dam height h_D has to be changed in the same way as h (Tab. 2). The results of this variation are presented in Fig. 6 and show a smaller difference between the 3-D-numerical simulation and the equations with a bigger still water depth h. For Fig. 7 freeboard f is varied between 0 and 8 m with a constant still water depth h. Based on this assumption, a smaller f also decreases the differences between the two concepts. In the case of $f = 0\,\text{m}$, the results corresponding to the overtopping volume V are nearly the same, only the run-up height R is higher in FLOW-3D than it is predicted by the equations based on Heller et al. (2009). Both mentioned variations are more theoretical. In a practical case the dam height h_D is fixed and the still water depth in the reservoir can be restricted in winter to reduce the potential damage. Therefore, further simulations are conducted, in which the freeboard is varied between 0 and 10 m and the water depth h in the range of 22 to 31.5 m. In order to be able to compare all tested combinations (including those with a fixed f and h; Tab. 2), the freeboard f divided by the still water depth h is used as the x axis in Fig. 8. This value reaches from 0.00 (no freeboard) to 0.45 [–]. In addition, only the primary impulse wave is examined to compare the overtopping volume V with the results of the formulas based on Heller et al. (2009).

A higher freeboard f or a smaller water depth h respectively leads to a smaller overtopping volume V. Both data sets can be approximated with a cubic function (Fig. 8). The difference between the values based on the formula and the 3-D-numerical simulation is small in case of a small freeboard and increases with an increasing ratio of f/h. This

analysis led to the assumption, that the found differences between formulas and 3-D-numerics are caused by the overfall process itself (the used dam face slope $\beta = 90°$ is an accepted border) and are not only a result of the chosen avalanche model in the simulation with FLOW-3D. Further research will be necessary, to investigate this hypothesis.

4.2.3 Width of the reservoir

The Excel-Tool based on Heller et al. (2009) also allows to simulate impulse waves propagating in 3-D. Therefore, the slide width b should be less than the reservoir width B. In contrast to the 2-D-version, which neglects the lateral movement, this option allows to include a radial wave propagation (Heller et al., 2009). For this reason, the computation of a more complex reservoir is possible. Within this context, a further parameter study is conducted, which focused on the reservoir width B. Figure 9 shows the widest of the investigated set-ups with a ratio of reservoir width B to slide width b of 3.75 [–] ($= 300\,\text{m}/80\,\text{m}$). Two guide walls are added to ensure that the model avalanche cannot expand. The width b of the inflowing model avalanche is thus held constant at a value of 80 m, which is equal to the reference case (Sect. 4.1).

The results of overtopping volume V based on the primary wave are shown in Fig. 10. The numerical values are compared with the 2-D-approach by Heller et al. (2009), which is independent of the parameter B. In addition to the numerical results with FLOW-3D, the overtopping volume V computed with the 3-D-option of the Excel-Tool is shown in this figure. For the reference case ($B/b = 1$ [–]), this option leads to a far smaller overtopping volume, as expected. If the ratio is increased ($B > b$) the measured volume of the 3-D-numerical simulation decreases and approaches the 3-D-option of the Excel-Tool by Heller et al. (2009). The differences get smaller between the formula based values and the results of the 3-D-numerical simulation correspond to an expanded reservoir width.

As mentioned in Sect. 3.3, the reference case with a reservoir width $B = b = 80$ m leads to a ratio η ($= L_R/B$) of 8.2 [–]. The laboratory tests at ETH Zürich were conducted in a channel with $\eta = 22$ [–]. In Fig. 10 the overtopping volume V of two exemplary simulations are added, for which the ratio η is 21.9 [–]. Therefore, the avalanche width b is reduced to

30 m as an additional verification of the 3-D-numerical simulations with the software FLOW-3D. In addition to $B/b = 1$ [–] the maximum ratio with $B/b = 3.73$ [–] ($= 112\,\mathrm{m}/30\,\mathrm{m}$) is also investigated. Depending on the overtopping volume V per m crest length, this change has no significant influence on the numerical results and this result in Fig. 10 confirms the statement in Sec. 3.3. Depending on the influence of reservoir width B, the results of Heller et al. (2009) can therefore be reproduced with the avalanche modelled with water.

5 Conclusions

The paper presents a new approach for simulating the impact of an avalanche into a reservoir with the 3-D-numerical software FLOW-3D. Water is placed in the release zone and only accelerated by gravity. The volume of the used water is identical to the melted snow (mass conservation) and the flow behaviour is also comparable to the avalanche simulation. Restarts of the model avalanche, for which the velocity of the inflowing water is set to zero, are used to calibrate the velocities with which the water reaches the reservoir (Sect. 3.1). After the calibration, the complete impact behaviour of the model avalanche is compared with the basic avalanche simulation. In all investigated cases a very good agreement could be found.

The advantages of this modelling concept are the limitation on two fluids (water and air) to simulate such an impact as well as the good adaptation of the avalanche onto the terrain. The latter can be a critical point, if simplified solid bodies are used to generate the impulse wave. By using 3-D-numerical simulations in general, complex terrains and reservoirs including spillways or other structures can be included in the investigation. Furthermore, reflexions and interactions of the impulse waves can be simulated as well as resulting influences on the downstream area of the dam.

The long standing research at ETH Zürich in the field of impulse waves led to generalised formulas to compute such an impact (Sect. 2.3). The findings based on the laboratory tests are summarised by Heller et al. (2009) and supported by an Excel-Tool. This notable approach is used to evaluate the numerical results based on the presented

modelling concept with FLOW-3D. Therefore, a simplified reference set-up in nature scale is investigated in detail. The comparison of the overtopping volume V over the dam caused by the primary wave shows a good agreement, although the 3-D-numerics reach a slightly higher value (Sect. 4.1). Further research should also use the available data of actual scale model tests to investigate the impact process and the wave propagation in the reservoir in detail. For the used test case, which is intended to be a prove of concept, the best agreement can be found if the freeboard f at the dam is small in relation to the still water depth h. The conducted parameter studies also include a variation of the reservoir width B with a fixed slide width b of the avalanche (Sect. 4.2). In this particular case, the results are compared with the computed values of the Excel-Tool by using the 3-D-options and also lead to a good agreement.

The comparison of the 3-D-numerical approach and the used formulas provided by ETH Zürich showed similar ouvertopping volumes for the investigated reference case and the conducted parameter studies. Hence, the presented model concept can help to quantify the impulse wave and its consequence for actual (complex) projects based on FLOW-3D. The extension of the parameter study (including the assumption that the slide thickness s of the avalanche is reduced in this concept) and the validation of the results with nature data should be part of further research.

Acknowledgements. The presented work mainly bases on third-party funded research. The authors want to thank different Austrian hydro power producers and FLOW-3D Germany for the support. The authors are grateful to the editor Thomas Glade and the two anonymous reviewers for their valuable comments.

References

Akgün, A.: Assessment of possible damaged areas due to landslide-induced waves at a constructed reservoir using empirical approaches: Kurtun (North Turkey) Dam reservoir area, Nat. Hazards Earth Syst. Sci., 11, 1341–1350, doi:10.5194/nhess-11-1341-2011, 2011.

Ataie-Ashtiani, B. and Shobeyri, G.: Numerical simulation of landslide impulsive waves by incompressible smoothed particle hydrodynamics, Int. J. Numer. Meth. Fl., 56, 209–232, doi:10.1002/fld.1526, 2008.

Ataie-Ashtiani, B. and Yavari-Ramshe, S.: Numerical simulation of wave generated by landslide incidents in dam reservoirs, Landslides, 8, 417–432, doi:10.1007/s10346-011-0258-8, 2011.

Capone, T., Panizzo, A., and Monaghan, J. J.: SPH modelling of water waves generated by submarine landslides, J. Hydraul. Res., 48, 80–84, doi:10.1080/00221686.2010.9641248, 2010.

Cascini, L., Cuomo, S., Pastor, M., Sorbino, G., and Piciullo, L.: SPH run-out modelling of channelised landslides of the flow type, Geomorphology, 214, 502–513, doi:10.1016/j.geomorph.2014.02.031, 2014.

Christen, M., Kowalski, J., and Bartelt, P.: RAMMS: numerical simulation of dense snow avalanches in three-dimensional terrain, Cold Reg. Sci. Technol., 63, 1–14, doi:10.1016/j.coldregions.2010.04.005, 2010.

Dai, Z., Huang, Y., Cheng, H., and Xu, Q.: 3D numerical modeling using smoothed particle hydrodynamics of flow-like landslide propagation triggered by the 2008 Wenchuan earthquake, Eng. Geol., 180, 21–33, doi:10.1016/j.enggeo.2014.03.018, 2014.

Dalban Canassy, P., Bauder, A., Dost, M., Fäh, R., Funk, M., Margreth, S., Müller, B., and Sugiyama, S.: Hazard assessment investigations due to recent changes in Triftgletscher, Bernese Alps, Switzerland, Nat. Hazards Earth Syst. Sci., 11, 2149–2162, doi:10.5194/nhess-11-2149-2011, 2011.

Dargahi, B.: Flow characteristics of bottom outlets with moving gates, J. Hydraul. Res., 48, 476–482, doi:10.1080/00221686.2010.507001, 2010.

Di Risio, M., De Girolamo, P., Bellotti, G., Panizzo, A., Aristodemo, F., Molfetta, M. G., and Petrillo, A. F.: Landslide-generated tsunamis runup at the coast of a conical island: new physical model experiments, J. Geophys. Res., 114, C01009, doi:10.1029/2008JC004858, 2009.

Erduran, K. S., Seckin, G., Kocaman, S., and Atabay, S.: 3D numerical modelling of flow around skewed bridge crossing, Engineering Applications of Computational Fluid Mechanics, 6, 475–489, doi:10.1080/19942060.2012.11015436, 2012.

Fach, S., Sitzenfrei, R., and Rauch, W.: Determining the spill flow discharge of combined sewer overflows using rating curves based on computational fluid dynamics instead of the standard weir equation, Water Sci. Technol., 60, 3035–3043, doi:10.2166/wst.2009.752, 2009.

Ferrand, M., Laurence, D. R., Rogers, B. D., Violeau, D., and Kassiotis, C.: Unified semi-analytical wall boundary conditions for inviscid, laminar or turbulent flows in the meshless SPH method, Int. J. Numer. Meth. Fl., 71, 446–472, doi:10.1002/fld.3666, 2013.

Flow Science, Inc.: FLOW-3D Version 11.0.3 User Manual, Santa Fe, USA, 2014.

Fritz, H. M.: Initial phase of landslide generated impulse waves, Mitteilungen 178, Versuchsanstalt für Wasserbau, Hydrologie und Glaziologie (VAW), ETH Zürich, 2002.

Fritz, H. M., Hager, W. H., and Minor, H.-E.: Landslide generated impulse waves. 1. Instantaneous flow fields, Exp. Fluids, 35, 505–519, doi:10.1007/s00348-003-0659-0, 2003a.

Fritz, H. M., Hager, W. H., and Minor, H.-E.: Landslide generated impulse waves. 2. Hydrodynamics impact craters, Exp. Fluids, 35, 520–532, doi:10.1007/s00348-003-0660-7, 2003b.

Fritz, H. M., Hager, W. H., and Minor, H.-E.: Near Field Characteristics of Landslide Generated Impulse Waves, Journal of Waterway, Port, Coastal, and Ocean Engineering, 130:6, 287–302, doi:10.1061/(ASCE)0733-950X(2004)130:6(287), 2004.

Fritz, H. M., Mohammed, F., and Yoo, J.: Lituya Bay landslide impact generated mega-tsunami 50th anniversary, Pure Appl. Geophys., 166, 153–175, doi:10.1007/s00024-008-0435-4 , 2009.

Fuchs, H., and Hager, W.: Scale Effects of Impulse Wave Run-Up and Run-Over, J. Waterway, Port, Coastal, Ocean Eng., 138(4), 303-–311, doi:10.1061/(ASCE)WW.1943-5460.0000138, 2012.

Fuchs, H., and Hager, W.: Solitary Impulse Wave Transformation to Overland Flow J. Waterway, Port, Coastal, Ocean Eng., 141(5), 304015004, doi:10.1061/(ASCE)WW.1943-5460.0000294, 2015.

Fuchs, H., Heller, V., and Hager, W.: Impulse wave run-over: experimental benchmark study for numerical modelling, Exp. Fluids, 49, 985–1004, doi:10.1007/s00348-010-0836-x, 2010.

Fuchs, H., Pfister, M., Boes, R., Perzlmaier, S., and Reindl, R.: Impulswellen infolge Lawineneinstoß in den Speicher Kühtai, WasserWirtschaft, 1–2, 54–60, 2011.

Fuchs, H., Winz, E., and Hager, W.: Underwater Landslide Characteristics from 2D Laboratory Modeling, J. Waterway, Port, Coastal, Ocean Eng., 139(6), 480–488, doi:10.1061/(ASCE)WW.1943-5460.0000201, 2013.

Gabl, R., Kapeller, G., and Aufleger, M.: Avalanche Impact into a Reservoir – Comparison of Numerical and Physical Model (Lawineneinstoß in einen Speichersee – Vergleich numerisches und physikalisches Modell), WasserWirtschaft, 5, 26–29, 2010.

Gabl, R., Gems, B., De Cesare, G., and Aufleger, M.: Contribution to Quality Standards for 3D-Numerical Simulations with FLOW-3D (Anregungen zur Qualitätssicherung in der 3-D-numerischen Modellierung mit FLOW-3D), WasserWirtschaft, 3, 15–20, 2014a.

Gabl, R., Gems, B., Plörer, M., Klar, R., Gschnitzer, T., Achleitner, S., and Aufleger, M.: Numerical simulations in hydraulic engineering, in: Computational Engineering, Dordrecht, Heidelberg, London, New York, Berlin, doi:10.1007/978-3-319-05933-4_8, 195–224, 2014b.

Gems, B., Wörndl, M., Gabl, R., Weber, C., and Aufleger, M.: Experimental and numerical study on the design of a deposition basin outlet structure at a mountain debris cone, Nat. Hazards Earth Syst. Sci., 14, 175–187, doi:10.5194/nhess-14-175-2014, 2014.

Grêt-Regamey, A. and Straub, D.: Spatially explicit avalanche risk assessment linking Bayesian networks to a GIS, Nat. Hazards Earth Syst. Sci., 6, 911–926, doi:10.5194/nhess-6-911-2006, 2006.

Heller, V.: Landslide generated impulse waves: Prediction of near field characteristics, Mitteilungen 204, Versuchsanstalt für Wasserbau, Hydrologie und Glaziologie (VAW), ETH Zürich, 2008.

Heller, V.: Scale effects in physical hydraulic engineering models, J. Hydraul. Res., 49, 293–306, doi:10.1080/00221686.2011.578914, 2011.

Heller, V. and Spinneken, J.: Improved landslide-tsunami prediction: Effects of block model parameters and slide model, J. Geophys. Res.-Oceans, 118, 1489–1507, doi:10.1002/jgrc.20099, 2013.

Heller, V. and Spinneken, J.: On the effect of the water body geometry on landslide–tsunamis: Physical insight from laboratory tests and 2D to 3D wave parameter transformation, Coastal Engineering, 104, 113–134, doi:10.1016/j.coastaleng.2015.06.006, 2015.

Heller, V., Hager, W. H., and Minor, H.-E.: Scale effects in subaerial landslide generated impulse waves, Exp. Fluids, 44, 691–703, doi:10.1007/s00348-007-0427-7, 2008a.

Heller, V., Hager, W. H., and Minor, H.-E.: Rutscherzeugte Impulswellen in Stauseen – Grundlagen und Berechnung, Manual für das Bundesamt für Energie BFE, Bern, 2008b.

Heller, V., Hager, W. H., and Minor, H.-E.: Landslide generated impulse waves in reservoirs – Basics and computation, Mitteilungen 211, Versuchsanstalt für Wasserbau, Hydrologie und Glaziologie (VAW), ETH Zürich, 2009.

Hirt, C. and Nichols, B.: Volume of Fluid (VOF) method for the dynamics of free boundaries, J. Comput. Phys., 39, 201–225, 1981.

Hübl, J., Hochschwarzer, M., Sereinig, N., and Wöhrer-Alge, M.: Alpine Naturgefahren – Ein Handbuch für Praktiker, Wildbach- und Lawinenverbauung Sektion Vorarlberg, Bregenz, available at: http://www.adaptalp.org/, last access: 05 May 2015, 2011.

Johnson, M. and Savage, B.: Physical and numerical comparison of flow over ogee spillway in the presence of tailwater, J. Hydraul. Eng.-ASCE, 132, 1353–1357, doi:10.1061/(ASCE)0733-9429(2006)132:12(1353), 2006.

Keiler, M., Sailer, R., Jörg, P., Weber, C., Fuchs, S., Zischg, A., and Sauermoser, S.: Avalanche risk assessment – a multi-temporal approach, results from Galtür, Austria, Nat. Hazards Earth Syst. Sci., 6, 637–651, doi:10.5194/nhess-6-637-2006, 2006.

Lo, D.-C., Liou, J.-S., and Chang, S. W.: Hydrodynamic performances of air–water flows in gullies with and without swirl generation vanes for drainage systems of buildings, Water, 7, 679–696, doi:10.3390/w7020679, 2015.

Meister, M., Burger, G., and Rauch, W.: On the Reynolds number sensitivity of smoothed particle hydrodynamics, J. Hydraul. Res., 52, 824–835, doi:10.1080/00221686.2014.932855, 2014.

Mohammed, F., and Fritz, H.W.: Physical modeling of tsunamis generated by three-dimensional deformable granular landslides, J. of Geophysical Research: Oceans, 117, 2156-2202, doi:10.1029/2011JC007850, 2012.

Müller, D. R.: Auflaufen und Überschwappen von Impulswellen an Talsperren, Mitteilungen 137, Versuchsanstalt für Wasserbau, Hydrologie und Glaziologie (VAW), ETH Zürich, 1995.

Panizzo, A., De Girolamo, P., Di Risio, M., Maistri, A., and Petaccia, A.: Great landslide events in Italian artificial reservoirs, Nat. Hazards Earth Syst. Sci., 5, 733–740, doi:10.5194/nhess-5-733-2005, 2005a.

Panizzo, A., De Girolamo, P., and Petaccia, A.: Forecasting impulse waves generated by subaerial landslides, J. Geophys. Res., 110, C12025, doi:10.1029/2004JC002778, 2005b.

Rastello, M., Ancey, C., Ousset, F., Magnard, R., and Hopfinger, E. J.: An experimental study of particle-driven gravity currents on steep slopes with entrainment of particles, Nat. Hazards Earth Syst. Sci., 2, 181–185, doi:10.5194/nhess-2-181-2002, 2002.

Sailer, R., Rammer, L., and Sampl, P.: Recalculation of an artificially released avalanche with SAMOS and validation with measurements from a pulsed Doppler radar, Nat. Hazards Earth Syst. Sci., 2, 211–216, doi:10.5194/nhess-2-211-2002, 2002.

Sampl, P. and Zwinger, T.: Avalanche simulation with SAMOS, Ann. Glaciol., 38, 393–398, doi:10.3189/172756404781814780, 2004.

Seibl, J., Gabl, R., Gems, B., and Aufleger, M.: 3-D-numerical Investigation of the Outflow-Hydrograph for Dam Failure (3-D-numerische Berechnung der Ausflusskurve infolge Staumauerversagen), WasserWirtschaft, 11, 28–33, 2014.

Shan, T. and Zhao, J.: A coupled CFD-DEM analysis of granular flow impacting on a water reservoir, Acta Mech., 225, 2449–2470, doi:10.1007/s00707-014-1119-z, 2014.

Teich, M., Fischer, J.-T., Feistl, T., Bebi, P., Christen, M., and Grêt-Regamey, A.: Computational snow avalanche simulation in forested terrain, Nat. Hazards Earth Syst. Sci., 14, 2233–2248, doi:10.5194/nhess-14-2233-2014, 2014.

Volk, G. and Kleemayr, K.: ELBA – Ein GIS-gekoppeltes Lawinensimulationsmodell Anwendungen und Perspektiven, Österreichische Zeitschrift für Vermessung und Geoinformation, 2/3, 84–92, 1999.

Waythomas, C. F., Watts, P., and Walder, J. S.: Numerical simulation of tsunami generation by cold volcanic mass flows at Augustine Volcano, Alaska, Nat. Hazards Earth Syst. Sci., 6, 671–685, doi:10.5194/nhess-6-671-2006, 2006.

Zweifel, A.: Impulswellen: Effekte der Rutschdichte und der Wassertiefe, Mitteilungen 186, Versuchsanstalt für Wasserbau, Hydrologie und Glaziologie (VAW), ETH Zürich, 2004.

Zweifel, A., Zuccala, D., and Gatti, D.: Comparison between computed and experimentally generated impulse waves, J. Hydraul. Eng.-ASCE, 133, 208–216, doi:10.1061/(ASCE)0733-9429(2007)133:2(208), 2007.

Table 1. Input paramter for the reference geometry based on the water slide.

parameter	value
slide width $b =$ reservoir width B	80 m
slide impact velocity v_s	40.4 m s^{-1}
bulk slide volume V_s	36 150 m^3
slide thickness s	6.35 m
bulk slide density $\rho_s = \rho_w$	1000 kg m^{-3}
bulk slide porosity n	0.01 %
slide impact angle α	40°
still water depth h	30 m
streamwise coordinate x	656 m
dam face slope β	90°
freeboard f	2 m
crest width b_k	3 m

Table 2. Input parameters for the variation and the results (run-up height R and overtopping volume V) for both modelling concepts.

freeboard f [m]	still water depth h [m]	dam height h_D [m]	f/h	R [m]		V [m^3 m^{-1}]	
				FLOW-3D	ETH	FLOW-3D	ETH
2	**30**	**32**	**0.07**	**15.7**	**15.2**	**487**	**431**
2	29	31	0.07	17.1	15.3	471	425
2	28	30	0.07	17.5	15.3	477	419
2	27	29	0.07	17.1	15.4	471	413
2	26	28	0.08	16.6	15.5	481	407
2	24	26	0.08	14.9	15.7	490	394
0	**30**	30	0.00	16.1	15.2	584	588
0.5	**30**	30.5	0.02	16.1	15.2	573	547
1	**30**	31	0.03	16.5	15.2	522	506
3	**30**	33	0.10	17.4	15.2	423	363
4	**30**	34	0.13	18.1	15.2	383	300
6	**30**	36	0.20	19.1	15.2	309	195
8	**30**	38	0.27	20.6	15.2	244	113
0.5	31.5	**32**	0.02	13.5	15.1	537	558
1	31	**32**	0.03	14.3	15.1	514	514
1.5	30.5	**32**	0.05	15.0	15.2	491	471
3	29	**32**	0.10	17.7	15.3	430	358
4	28	**32**	0.14	18.3	15.3	391	293
5	27	**32**	0.19	17.7	15.4	344	237
6	26	**32**	0.23	18.8	15.5	310	188
8	24	**32**	0.33	17.3	15.7	241	111
10	22	**32**	0.45	17.5	15.9	186	58

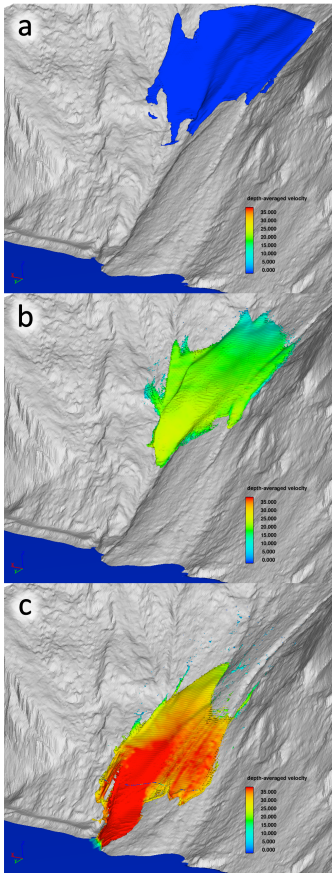

Figure 1. Exemplary results of a simulation with FLOW-3D (including added original stl-geometry) of a stopped and restarted avalanche model at **(a)** 0 s, **(b)** 4 s and **(c)** 8 s after the restart and before it reaches the reservoir – coloured by the depth-averaged velocities in [$\mathrm{m\,s^{-1}}$] with a range of 0 to 35 $\mathrm{m\,s^{-1}}$.

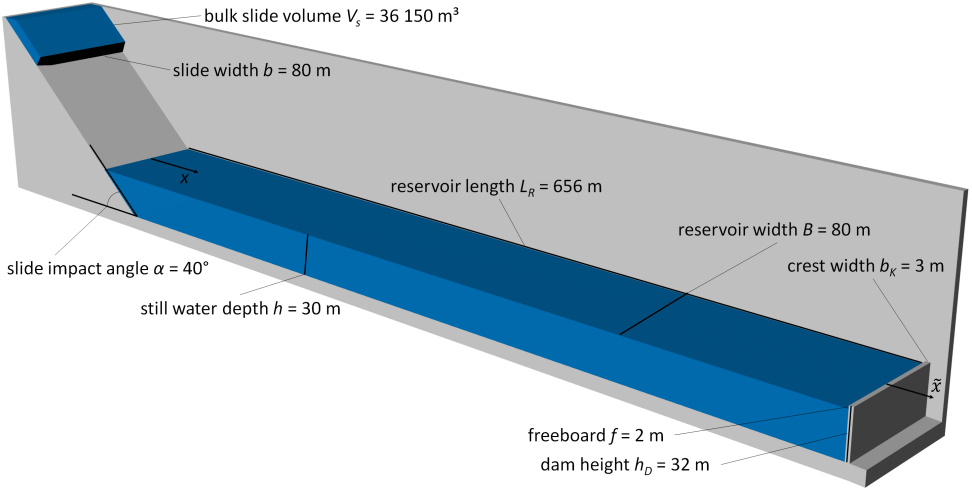

Figure 2. Reference geometry including the initial condition at time = 0 s.

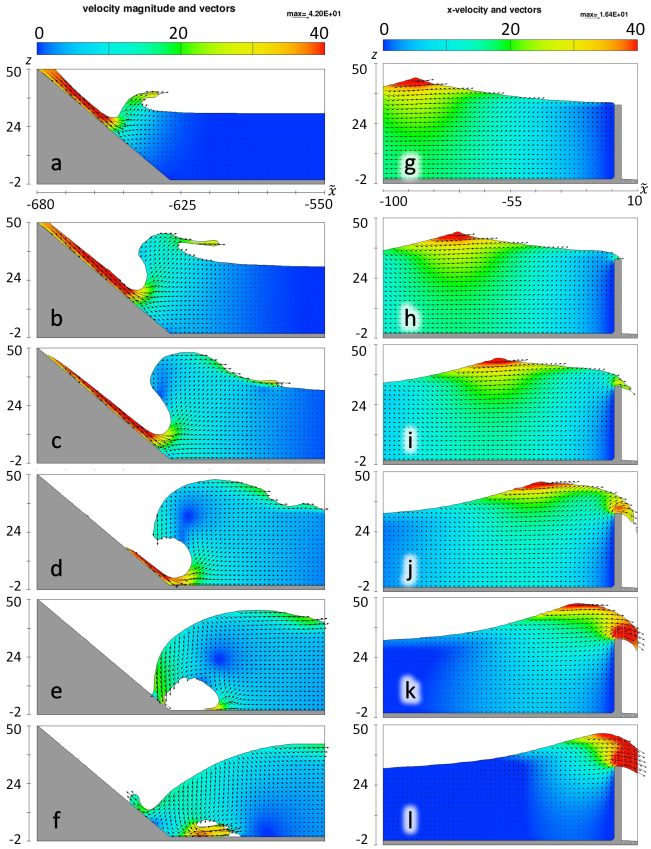

Figure 3. Exemplary results of the reference case – left column **(a)** to **(f)**: impact of the avalanche starting at 1 s after the start of the simulation; coloured by the velocity magnitude with a fixed upper value of 40 m s^{-1} – right column **(g)** to **(l)**: overtopping starting at 30.4 s (Δt between each picture is 1 s); coloured by the x velocity with a fixed upper value of 10 m s^{-1} (vectors show the 2-D-velocity – length dimension of the axis in [m]).

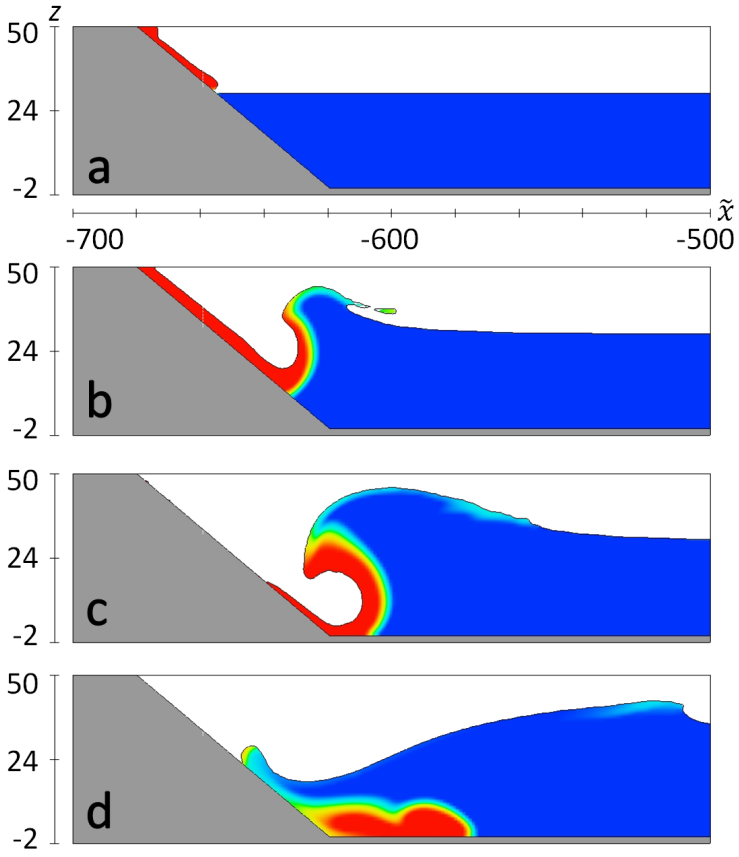

Figure 4. Impact of the avalanche at time **(a)** 4.6 s, **(b)** 6.6 s, **(c)** 8.6 s, **(d)** 11.6 s – water, which is used as the model avalanche, is marked red and water in the reservoir blue – all length dimension in [m].

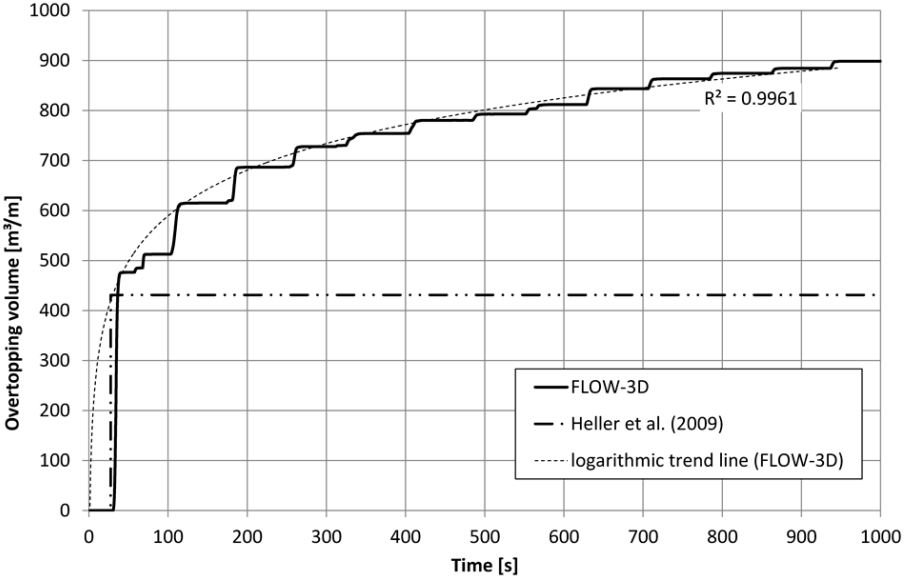

Figure 5. Accumulation of the overtopping volume V over the dam for the reference geometry including a logarithmic trendline for the approximation of the FLOW-3D simulation.

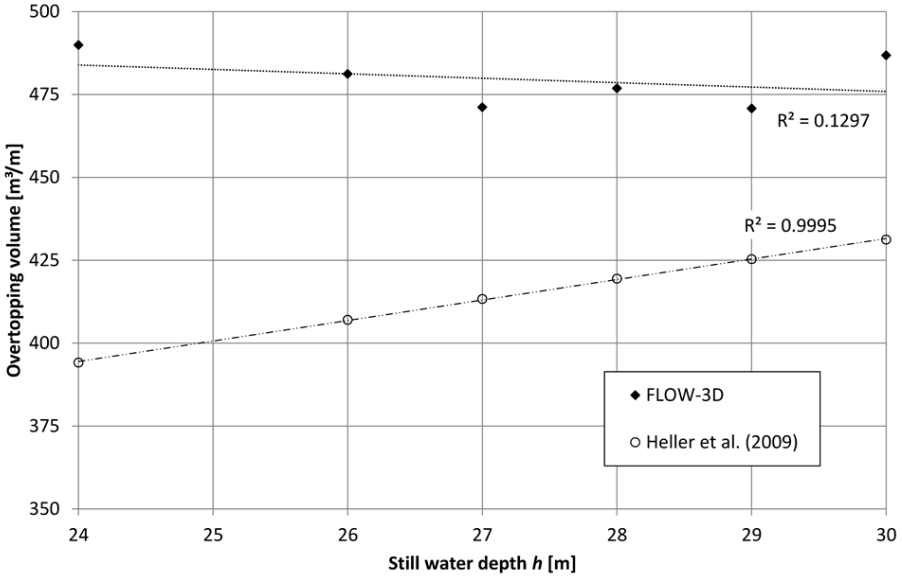

Figure 6. Overtopping volume V depending on a variation of the still water depth h including trendlines with a fixed freeboard $f = 2\,\text{m}$.

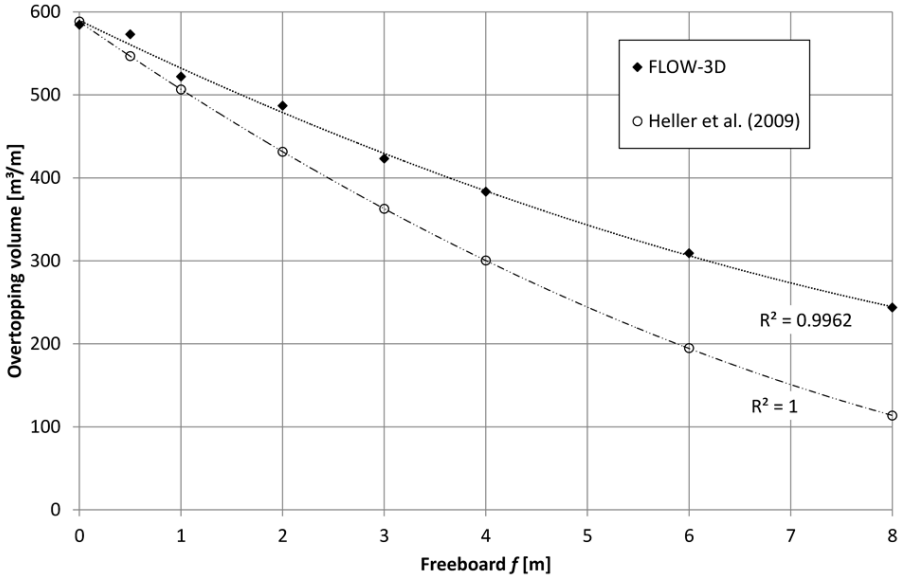

Figure 7. Overtopping volume V depending on the freeboard f including trendlines with a fixed still water depth $h = 30$ m.

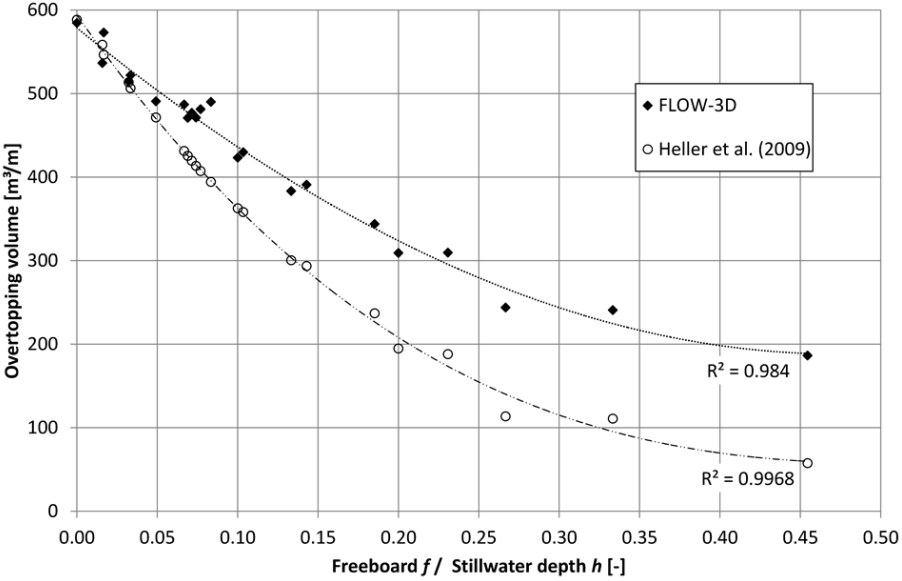

Figure 8. Overtopping volume V depending on the ratio freeboard f to still water depth h including trendlines – Results of the complete variation presented in Tab. 2

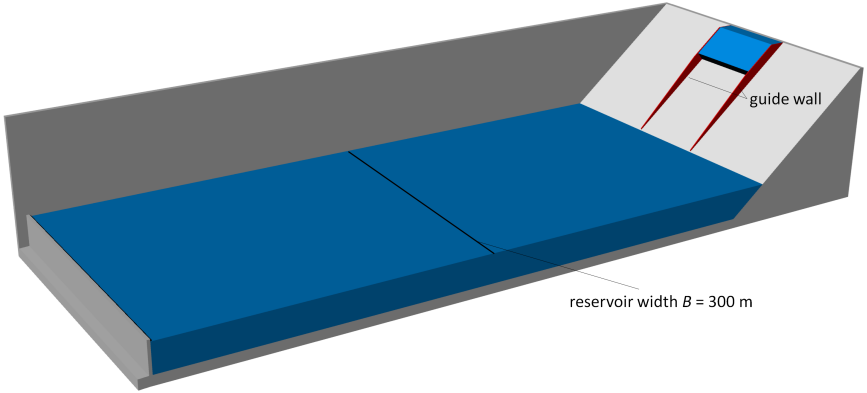

Figure 9. Initial condition for simulation with $B = 300\,\mathrm{m}$ and $b = 80\,\mathrm{m}$ – guide walls are coloured in red.

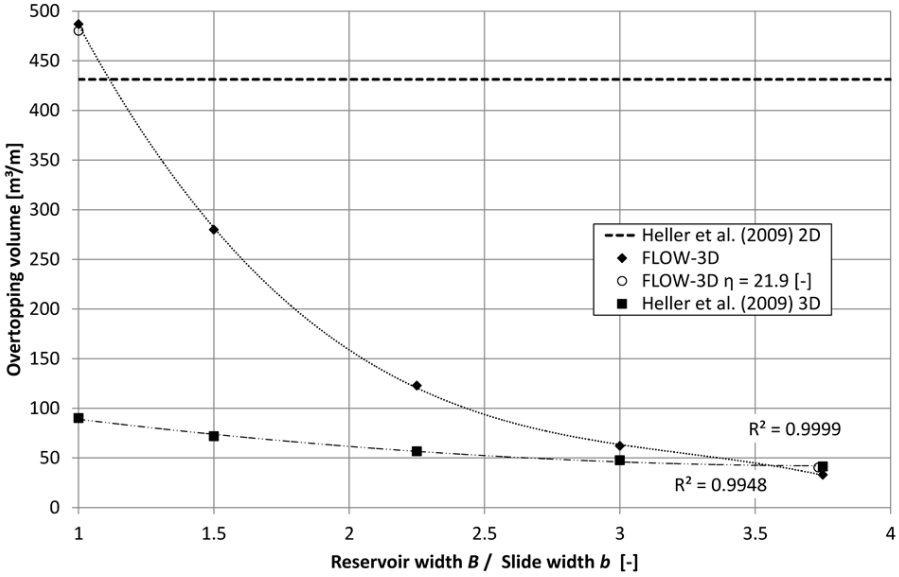

Figure 10. Overtopping volume V depending on the slide width b and reservoir width B including trendlines.